Supporting information for

Simultaneous observation of halogen-lone pair and halogen-π interactions of ferrocene derivatives under cryogenic conditions

Nora M. Kreienborg,[a] Felix Otte,[b] Carsten Strohmann,[b] Christian Merten*[a]

[a)] Ruhr Universität Bochum
Fakultät für Chemie und Biochemie, Organische Chemie II
Universitätsstraße 150
44801 Bochum, Germany
christian.merten@ruhr-uni-bochum.de
www.mertenlab.de

[b)] Technische Universität Dortmund
Fakultät für Chemie und Chemische Biologie, Anorganische Chemie
Otto-Hahn-Straße 6
44227 Dortmund, Germany

1. Additional Figures and Tables

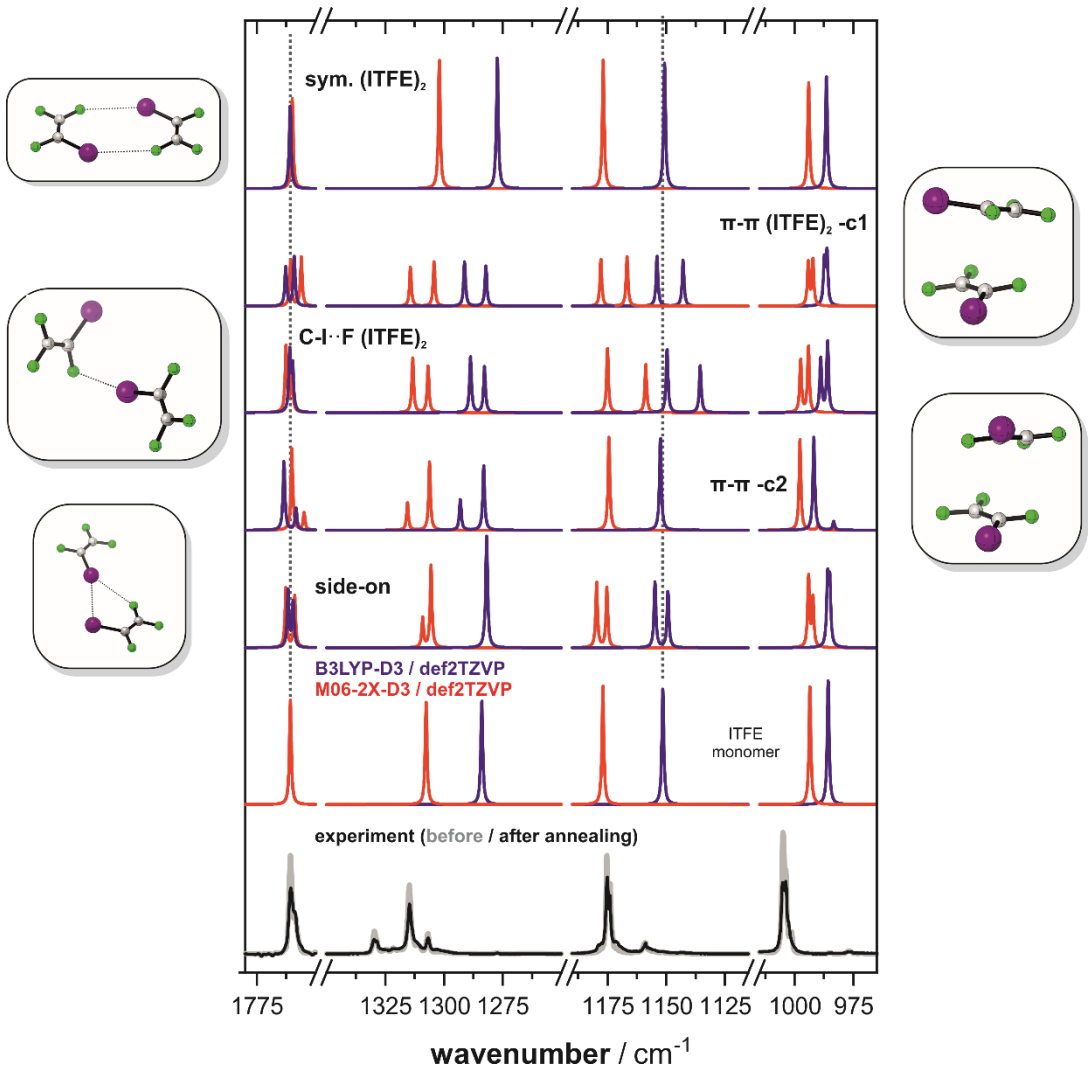

Figure S1. Comparison of the experimental MI-IR spectra of ITFE in Argon matrix with those computed for ITFE and $(ITFE)_2$ at B3LYP-D3/def2TZVP and M06-2X-D3/def2TZVP level of theory. Details on conformer energies are collected in Table S1 below. Please note that the frequency scaling factors were chosen to match the experimental band position of the C=C stretching vibration of ITFE. The side-on structure is considered to match best with the experiment as it shows a splitting into two bands for the C=C (~1760 cm^{-1}) and the C-F strecthing mode (~1175 cm^{-1}) and a weak red-shift of the C-F stretching in $=CF_2$ at ~1315 cm^{-1}. In the π-π-$(ITFE)_2$-c1, both aforementioned C-F modes split, which is not seen in the experiment (there are no new bands in the =CF2 stretching region).

Table S1. Relative energies of the five considered dimers of ITFE in kcal/mol.

	B3LYP-D3 / def2TZVP			Single point B3LYP-D3 / def2QZVPP			B3LYP-D3BJ / def2TZVP		
	ΔE_{pot}	ΔE_{ZPC}	ΔH	ΔE_{pot}	ΔE_{ZPC}	ΔH	ΔE_{pot}	ΔE_{ZPC}	ΔH
π-π $(ITFE)_2$ -c1	0.00	0.00	0.00	0.0	0.0	0.0	0.0	0.0	0.0
π-π $(ITFE)_2$ -c2	0.4	0.4	0.4	0.5	0.4	0.5	0.6	0.6	0.6
C-I··F	1.7	1.6	1.7	1.5	1.4	1.5	1.6	1.5	1.6
Side-on $(ITFE)_2$	2.3	2.0	1.8	1.9	1.7	1.5	1.7	1.5	1.3
symmetric $(ITFE)_2$	2.4	2.2	2.0	2.1	1.8	1.6	2.2	2.0	1.8

	M06-2X-D3 / def2TZVP			Single point M06-2X-D3 / def2QZVPP		
	ΔE_{pot}	ΔE_{ZPC}	ΔH	ΔE_{pot}	ΔE_{ZPC}	ΔH
π-π $(ITFE)_2$ -c1	0.0	0.0	0.0	0.0	0.0	0.0
π-π $(ITFE)_2$ -c2	0.6	0.6	0.6	0.6	0.6	0.6
C-I··F	2.4	2.3	2.4	2.2	2.0	2.1
Side-on $(ITFE)_2$	2.9	2.7	2.5	2.4	2.2	2.0
symmetric $(ITFE)_2$	3.3	3.0	3.2	2.9	2.6	2.8

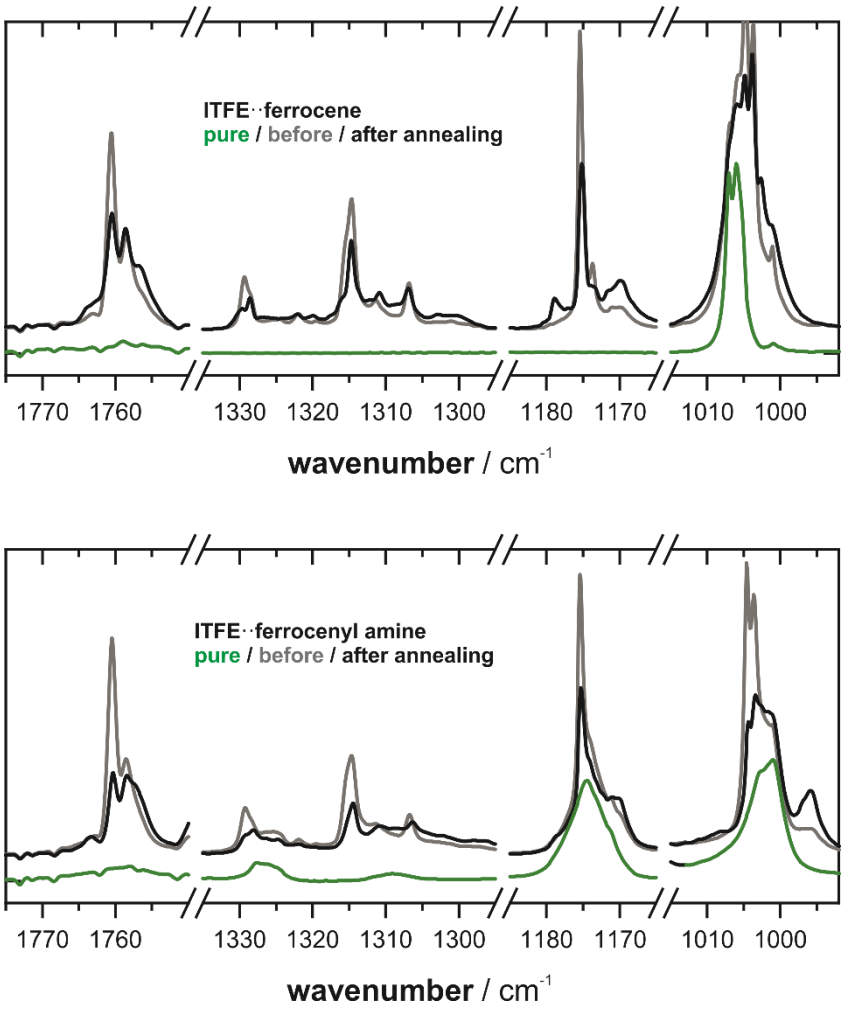

Figure S2. The matrix isolation spectra of ferrocene··ITFE and (N,N-dimethyl ferrocenyl amine)··ITFE in the range of the four main ITFE bands.

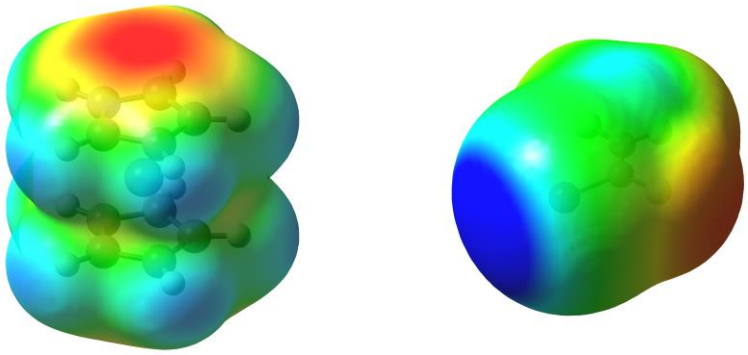

Figure S3. Electrostatic potential maps of ferrocene and ITFE obtained mapping the electrostatic potential on the electron density using iso-values of 6e-4 and 1e-5 on a scale from -2.5e-2(red) to 2.5 e-2 (blue) and -1e-2 (red) to 1e-2 (blue).

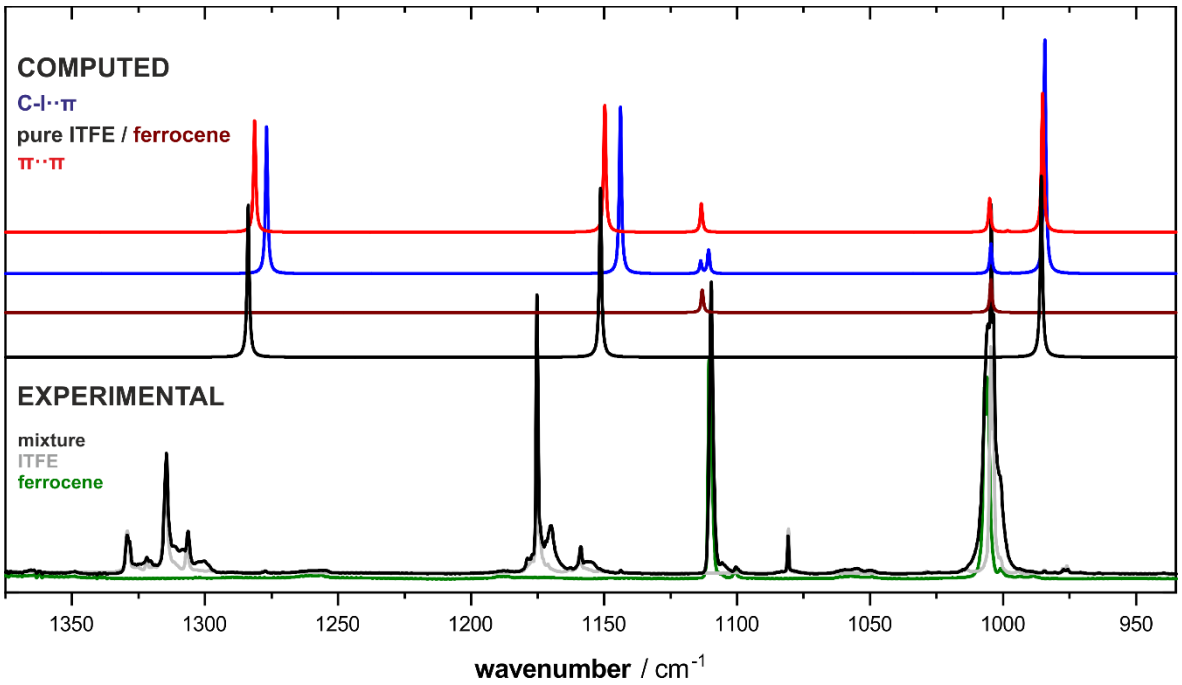

Figure S4. Comparison of the experimental MI-IR spectra of ferrocene/ITFE in Argon matrix with those computed for ferrocene··ITFE.

Table S2. Computed relative enthalpies of ferrocenyl amine and its XB-complex with ITFE computed at difference levels of theory. Energies are given in kcal/mol.

		B3LYP-D3 / def2TZVP			Single point B3LYP / def2QZVPP			M062X-D3 / def2TZVP			Single point M062X / def2QZVPP		
		ΔE_{pot}	ΔE_{ZPC}	ΔH	ΔE_{pot}	ΔE_{ZPC}	ΔH	ΔE_{pot}	ΔE_{ZPC}	ΔH	ΔE_{pot}	ΔE_{ZPC}	ΔH
C1		0.00	0.18	0.15	0.00	0.18	0.15	0.00	0.00	0.00	0.00	0.06	0.02
C2		0.04	**0.00**	0.00	0.03	0.00	0.00	0.22	0.02	0.05	0.14	0.00	0.00
C1	C-I··N	0.00	0.00	0.00	0.00	0.00	0.00	0.23	0.05	0.08	0.19	0.01	0.04
C2	C-I··N	0.09	0.26	0.25	0.07	0.24	0.23	0.00	0.00	0.00	0.00	0.00	0.00
C1	C-I··π	4.22	4.01	4.13	4.25	4.03	4.15	3.04	2.85	2.92	3.09	2.90	2.97
C2	C-I··π	5.70	5.07	5.36	5.62	4.99	5.28	4.82	4.23	4.49	4.69	4.10	4.36
C1	π··π	4.11	3.81	3.89	4.48	4.18	4.26	3.24	3.08	3.03	3.54	3.38	3.33
C2	π··π	4.38	4.24	4.33	4.81	4.67	4.76	3.11	3.05	3.00	3.57	3.51	3.46

Tabl. S3. Formation enthalpies of (ferrocenyl amine)··ITFE complexes obtained by $\Delta H_{formation}$ = H(C***x*** XBonded) – H(C***x***) – H(ITFE) with ***x*** indicating the pure donor's conformer. Energies are in kcal/mol.

		$\Delta H_{formation}$	
		B3LYP-D3	**M06-2X-D3**
C1	C-I··N	-8.91	-8.13
C2	C-I··N	-8.8	-8.16
C1	C-I··π	-3.55	-3.72
C2	C-I··π	-4.93	-5.24
C1	π··π	-5.02	-5.19
C2	π··π	-4.73	-5.16

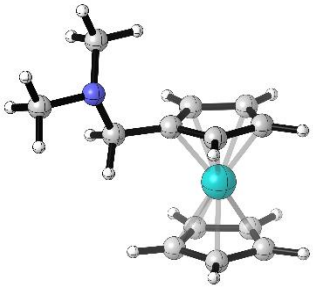

Ferrocenyl amine C1 (0.00)

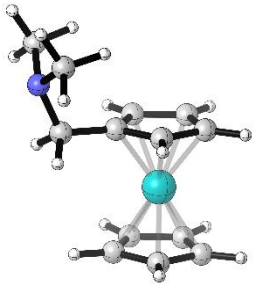

Ferrocenyl amine C2 (0.15)

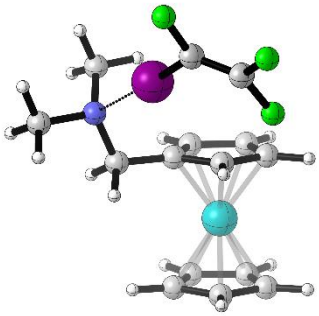

C1 (C-I··N)

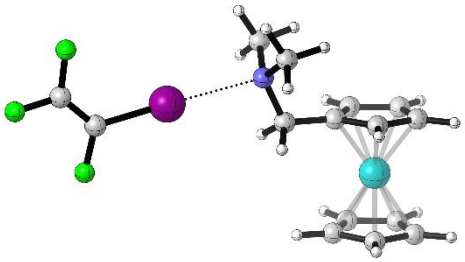

C2 (C-I··N)

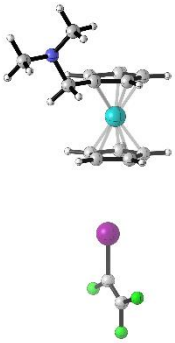

C1 (C-I··π) preferred to bottom Cp

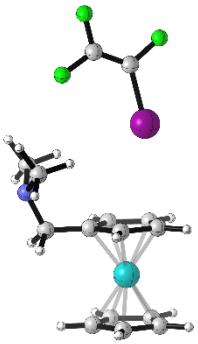

C2 (C-I··π) preferred to top Cp

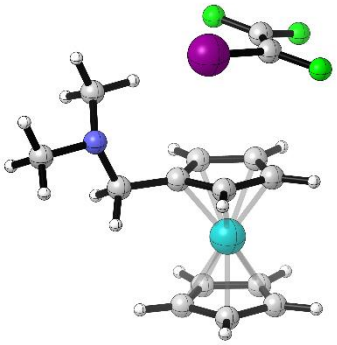

C1 (π··π)

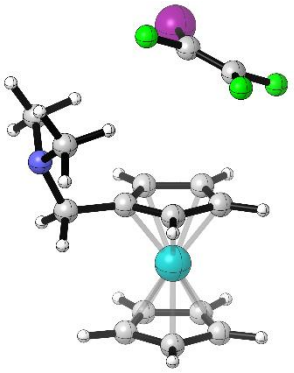

C2 (π··π)

Figure S5. Structures of the computed (ferrocenyl amine)··ITFE complexes. For the (ferrocenyl amine) monomers, the relative ΔH is given in parenthesis.

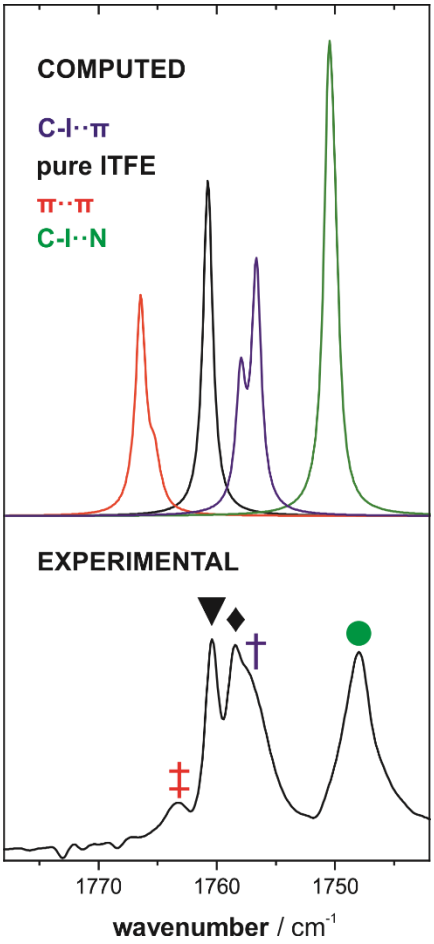

Figure S6. Comparison of the experimental MI-IR spectra of ferrocenyl amine/ITFE in Argon matrix with those computed for (ferrocenyl amine)··ITFE at B3LYP-D3/def2TZVP level of theory.

2. Experimental and computational details

ITFE was purchased from ABCR, Germany. All other compounds were purchased from Sigma Aldrich, Germany. All substances were used without further purification. Xenon gas (4.8, halogen-free) and Argon gas (99.9%) were obtained from AirLiquide.

Cryosolutions experiments

A stainless-steel IR transmission cell with BaF_2 windows and 7 mm pathlength was used. The cell was connected to a gas manifold. For the experiments with ferrocene and ferrocenyl amine, the compounds (exact amounts cf. Table S3) were dissolved in pentane and injected into the cell. The pentane was removed under reduced pressure at room temperature and pressurized by addition of Xenon gas, or it was continued with the sample preparation of ITFE. For the measurements of mixtures with ITFE, gas mixtures of ITFE with xenon were prepared at room temperature (p(ITFE) = 0.55 mbar = ~1.7 mol; $p_{Xe} \approx 3.75$ bar). While still connected to the gas manifold, the transmission cell was cooled down to 173 K with a Janis ST100 liquid-nitrogen cryostat, which led to partial condensation of the gas mixture and a reduction of the system pressure. The system was subsequently pressurized to a total system pressure of 3.5, 3.75 and 4.0 bar respectively by addition of Xenon gas.

Table S4. Experimental conditions for cryosolutions experiments

experiment	p(ITFE)/n(ITFE)	m(compound)/n(compound)	p(Xe)	T
ITFE	0.55 mbar / 1.7 µmol	- n/a -	4 bar	173
Ferrocene	- n/a -	2.0 mg/ 10.8 µmol	4 bar	178
Ferrocene + ITFE	0.55mbar/ 1.7 µmol	2.0 mg /10.8 µmol	4 bar	173
Ferrocenyl amine	- n/a -	1.19 mg/5.1 µmol	3.75 bar	173
Ferrocenyl amine + ITFE	0.545 mbar/ 1.7 µmol	1.2mg /5.1µmol	3.5 bar	173

Matrix isolation experiments

Argon matrices were obtained on a BaF_2 window held at a temperature of 20 K and utilizing an argon flow of 1.66 sccm. In case of ferrocene, the sample was sublimed from a previously degassed sample flask at a temperature of 55°C. Ferrocenyl amine was evaporated sublimated from a previously degassed sample flask at a temperature of 50°C. In both experiments, all transfer lines to the cold head were heated to 5°C above the sample temperature by means of a heating tap. For all experiments with ITFE, a gas mixture of ITFE and argon (the matrix host) was prepared with an approximate ratio of 1:1800 (ITFE:Argon). Annealing was carried out by slowly heating the matrix to 35 K and completed when no change of the IR spectrum could be observed anymore.

Table S5. Experimental conditions for matrix isolation experiments

experiment	Duration of depositon	Deposition temperature	Gas(mixture)	Sample
ITFE	3:02h	20K	1.1 : 1850 mbar	X
Ferrocene	48min	20K		55°C
Ferrocene + ITFE	49 min	20K	1.1 : 1813 mbar	55°C
Ferrocenyl amine	3:38h	20K		50°C
Ferrocenyl amine + ITFE	2:26h	20K	1 : 1809 mbar	50°C

Computational details

All calculations were carried out using Gaussian 09 Rev E.01,[1] three-dimensional structures were rendered using CylView.[2] For all calculations, dispersion was accounted for by employing the D3 (and in case of B3LYP also D3BJ) correction.[3] IR spectra were simulated by assigning a Lorentzian band width of 0.5 cm^{-1} half-width at half-height to the computed dipole strength. The frequency scaling factor, that is employed to account for deviations in frequencies due to the applied harmonic approximation, was set to 0.979 (B3LYP-D3) and 0.944 (M06-2X-D3) in order to match the experimental band position of the C=C stretching vibration of ITFE.

1. Gaussian 09, Rev E.01, M. J. Frisch, G. W. Trucks, H. B. Schlegel, G. E. Scuseria, M. A. Robb, J. R. Cheeseman, G. Scalmani, V. Barone, B. Mennucci, G. A. Petersson, H. Nakatsuji, M. Caricato, X. Li, H. P. Hratchian, A. F. Izmaylov, J. Bloino, G. Zheng, J. L. Sonnenberg, M. Hada, M. Ehara, K. Toyota, R. Fukuda, J. Hasegawa, M. Ishida, T. Nakajima, Y. Honda, O. Kitao, H. Nakai, T. Vreven, J. J. A. Montgomery, J. E. Peralta, F. Ogliaro, M. Bearpark, J. J. Heyd, E. Brothers, K. N. Kudin, V. N. Staroverov, T. Keith, R. Kobayashi, J. Normand, K. Raghavachari, A. Rendell, J. C. Burant, S. S. Iyengar, J. Tomasi, M. Cossi, N. Rega, J. M. Millam, M. Klene, J. E. Knox, J. B. Cross, V. Bakken, C. Adamo, J. Jaramillo, R. Gomperts, R. E. Stratmann, O. Yazyev, A. J. Austin, R. Cammi, C. Pomelli, J. W. Ochterski, R. L. Martin, K. Morokuma, V. G. Zakrzewski, G. A. Voth, P. Salvador, J. J. Dannenberg, S. Dapprich, A. D. Daniels, O. Farkas, J. B. Foresman, J. V. Ortiz, J. Cioslowski and D. J. Fox, Wallingford CT, USA, 2013
2. CYLview 1.0b, C. Y. Legault, Université de Sherbrooke, 2009
3. S. Grimme, *Chem. Eur. J.*, 2012, **18**, 9955-9964.

3. Crystallographic study

Crystals of the adduct (ferrocenyl amine)-ITFE were grown under exclusion of air and moisture by first dissolving ITFE (0.05 mL, 0.50 mmol, 1.00 eq.; pre-cooled to -40 °C) in dry n-pentane at -40 °C. Afterwards, N,N-dimethyl ferrocenyl amine (0.2 mL, 1.00 mmol, 2.00 eq.) was added. The sample was first kept in the -30 °C freezer, then moved to the -80 °C freezer until yellow plates formed.

A suitable crystal was selected and analyzed on a Bruker APEX-II CCD diffractometer. The crystal was kept at 100 K during data collection. Using Olex2[4], the structure was solved with the XT structure solution program[5] using Intrinsic Phasing and refined with the XL refinement package[6] using Least Squares minimisation.

4. O.V. Dolomanov et al., *J. Appl. Cryst.* 2009, **42**, 339-341.
5. G. M. Sheldrick, *Acta Cryst.*, 2015, **A71**, 3-8.
6. G. M. Sheldrick, *Acta Cryst.* 2008, **A64**, 112-122.

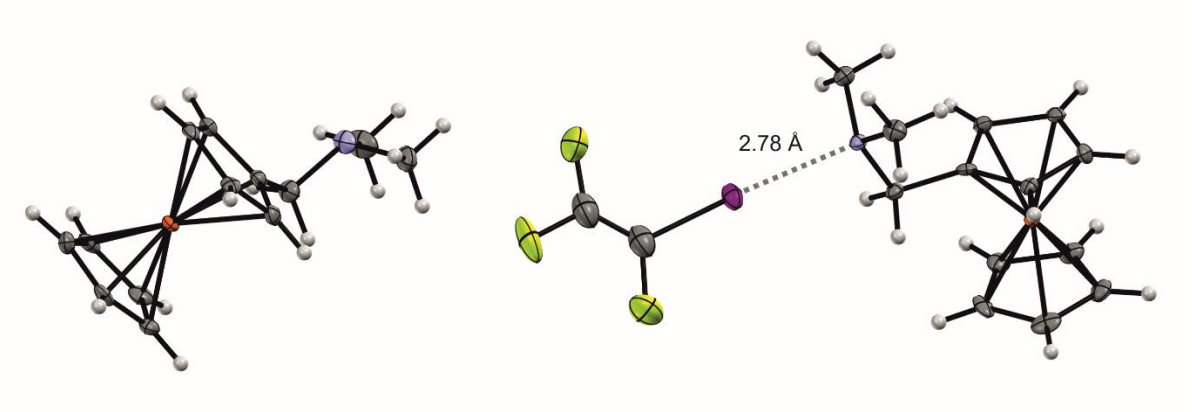

The addition of excess ferrocenyl amine led to the formation of crystals with a 2:1 ratio of XB-acceptor and -donor. The XB is formed with ferrocenyl amine in C2 conformation (cf. Fig. S5), while the other ferrocenyl amine adopts C1.

Table S6. Crystal data and structure refinement.

CCSD no.	2252978
Empirical formula	$C_{28}H_{34}F_3Fe_2IN_2$
Formula weight	694.17
Temperature/K	100
Crystal system	orthorhombic
Space group	$P2_12_12_1$
a/Å	5.7701(4)
b/Å	11.1748(8)
c/Å	42.916(3)
α/°	90
β/°	90
γ/°	90
Volume/Å^3	2767.2(3)
Z	4
ρ_{calc}g/cm^3	1.666
μ/mm^{-1}	2.204
F(000)	1392.0
Crystal size/mm^3	0.306 × 0.236 × 0.172
Radiation	MoKα (λ = 0.71073)
2Θ range for data collection/°	4.626 to 53.998
Index ranges	$-7 \leq h \leq 7$, $-15 \leq k \leq 15$, $-57 \leq l \leq 58$
Reflections collected	5989
Independent reflections	5989 [R_{int} = 0.0612, R_{sigma} = 0.0281]
Data/restraints/parameters	5989/0/329
Goodness-of-fit on F^2	1.146
Final R indexes [I>=2σ (I)]	R_1 = 0.0327, wR_2 = 0.0677
Final R indexes [all data]	R_1 = 0.0366, wR_2 = 0.0687
Largest diff. peak/hole / e Å^{-3}	1.67/-0.60
Flack parameter	-0.010(9)

Table S7. Fractional Atomic Coordinates ($\times 10^4$) and Equivalent Isotropic Displacement Parameters ($Å^2 \times 10^3$). U_{eq} is defined as 1/3 of of the trace of the orthogonalised U_{IJ} tensor.

Atom	*x*	*y*	*z*	U(eq)
I1	5567.3(7)	7108.1(3)	5644.5(2)	22.58(9)
Fe1	7153.3(12)	8459.2(6)	7161.6(2)	10.07(14)
F1	1743(8)	5739(4)	5342.7(11)	52.9(12)
F2	3714(9)	5288(4)	4793.2(9)	53.8(13)
F3	6918(9)	6219(5)	4935.4(11)	66.2(15)
N1	7321(7)	8553(4)	6116.4(9)	12.8(8)
C1	7438(8)	8839(4)	6696.4(11)	11.0(9)
C2	9676(9)	8862(4)	6841.3(11)	13(1)
C3	9648(10)	9738(4)	7082.1(11)	15(1)
C4	7371(9)	10262(4)	7087.8(12)	16.2(11)
C5	6036(9)	9713(4)	6848.2(11)	11.7(10)
C6	5683(11)	6801(4)	7197.3(12)	19.8(11)
C7	7909(10)	6805(4)	7338.2(13)	19.3(11)
C8	7872(10)	7676(5)	7581.3(12)	17.6(11)
C9	5645(11)	8204(4)	7588.6(11)	18.9(11)
C10	4309(11)	7660(5)	7350.2(12)	21.0(11)
C11	6741(8)	8062(4)	6425.1(11)	13.1(10)
C12	9811(9)	8668(5)	6067.7(12)	17.2(11)
C13	6176(10)	9703(4)	6058.5(12)	17.7(11)
C14	3948(13)	6127(5)	5284.1(15)	35.5(16)
C15	4805(15)	5898(6)	5021.3(17)	41.2(18)
Fe2	6128.1(12)	1314.2(6)	3591.8(2)	10.38(15)
N2	9959(8)	2753(4)	4401.2(10)	21.3(10)
C16	7679(9)	2313(4)	3929.8(11)	13.4(10)
C17	5407(9)	2754(4)	3866.8(11)	14.6(9)
C18	5324(9)	3095(4)	3545.0(11)	13.7(10)
C19	7542(9)	2851(5)	3412.3(11)	16.3(10)
C20	8976(9)	2382(4)	3649.5(11)	14.7(10)
C21	5774(10)	-376(4)	3773.1(13)	19.5(11)
C22	3597(9)	83(4)	3673.6(12)	16.6(11)
C23	3705(9)	339(4)	3351.5(13)	17.0(11)
C24	5986(10)	45(4)	3249.5(13)	18.5(11)
C25	7246(10)	-396(4)	3507.0(13)	18.0(11)
C26	8589(10)	1849(5)	4234.2(12)	18.3(11)
C27	11279(11)	2194(6)	4650.0(14)	32.7(14)
C28	8431(11)	3677(5)	4527.2(13)	27.4(13)

Table S8. Anisotropic Displacement Parameters ($Å^2 \times 10^3$). The Anisotropic displacement factor exponent takes the form: $-2\pi^2[h^2a^{*2}U_{11}+2hka^*b^*U_{12}+\ldots]$.

Atom	U_{11}	U_{22}	U_{33}	U_{23}	U_{13}	U_{12}
I1	31.7(2)	19.52(16)	16.52(16)	-0.39(14)	-3.54(16)	-2.14(16)
Fe1	11.5(3)	10.3(3)	8.4(3)	0.4(2)	1.0(3)	-0.5(3)
F1	40(3)	66(3)	53(3)	-15(2)	-3(2)	-21(2)
F2	90(4)	37(2)	34(2)	-13.9(17)	-24(2)	-4(2)
F3	69(3)	82(4)	48(3)	-32(3)	24(3)	-26(3)
N1	14(2)	15(2)	10(2)	0.6(16)	1.8(16)	-4.2(17)
C1	8(2)	12(2)	13(2)	4.1(17)	1.8(19)	-2.3(18)
C2	11(2)	16(2)	13(2)	0.6(17)	1(2)	-0.7(19)
C3	15(2)	17(2)	12(2)	1.1(18)	2(2)	-7(2)
C4	19(3)	10(2)	19(3)	-3.6(18)	3(2)	-1(2)
C5	14(3)	10(2)	11(2)	2.2(17)	2(2)	1.4(18)
C6	34(3)	9(2)	16(2)	2.8(17)	-2(3)	-8(2)
C7	25(3)	12(3)	21(3)	4.8(19)	5(2)	-1(2)
C8	16(3)	23(3)	14(2)	5.9(19)	-1(2)	1(2)
C9	24(3)	21(3)	12(2)	3.2(17)	5(2)	1(2)
C10	20(3)	27(3)	16(2)	15(2)	0(2)	2(2)
C11	15(2)	12(2)	13(2)	1.4(18)	4.0(19)	0.0(18)
C12	17(3)	19(2)	16(2)	-1(2)	3(2)	-2(2)
C13	19(3)	18(3)	16(3)	4.1(19)	-3(2)	0(2)
C14	49(4)	26(3)	32(4)	-1(2)	-6(3)	-4(3)
C15	59(5)	28(3)	36(4)	-5(3)	-6(4)	-4(3)
Fe2	10.7(3)	8.1(3)	12.3(3)	-0.4(2)	-1.2(3)	-0.8(2)
N2	24(3)	27(2)	13(2)	2.5(18)	-4.0(17)	-5.8(19)
C16	14(2)	10(2)	16(2)	-2.2(18)	-0.6(19)	-2.6(19)
C17	16(2)	11(2)	17(2)	-4.2(18)	0(2)	1(2)
C18	19(2)	9(2)	13(2)	3.8(17)	0(2)	-3.1(19)
C19	26(3)	9(2)	14(2)	-0.5(19)	2(2)	-7(2)
C20	16(3)	12(2)	16(2)	-3.6(17)	1(2)	-3.5(18)
C21	22(3)	11(2)	25(3)	5.2(19)	-2(2)	-3(2)
C22	17(3)	12(2)	21(3)	-0.6(19)	4(2)	-5.2(19)
C23	16(3)	14(2)	21(3)	-4.7(19)	-7(2)	-4(2)
C24	21(3)	15(2)	20(3)	-7.0(19)	4(2)	-1(2)
C25	13(3)	10(2)	31(3)	-5(2)	-4(2)	-1.0(19)
C26	21(3)	20(3)	14(2)	1.6(18)	-2(2)	-2(2)
C27	33(3)	43(4)	22(3)	8(3)	-13(3)	-10(3)
C28	39(4)	27(3)	16(3)	-4(2)	3(2)	-9(3)